Influence of clearance flow on disk friction loss in low specific speed hydraulic machines

IOP Conf. Series: Earth and Environmental Science **240** (2019) 032043 doi:10.1088/1755-1315/240/3/032043

Influence of clearance flow on disk friction loss in low specific speed hydraulic machines

Ryutaro Ujiie[1], Asuma Ichinose[1], Yohei Nakamura[1], Kazuyoshi Miyagawa[2], Takeshi Sano[3]

[1] Department of Applied Mechanics, Waseda University, Tokyo, 1690072, Japan
[2] Department of Applied Mechanics and Aerospace Engineering, Waseda University, Tokyo, 1690072, Japan
[3] Fluid Dynamics No.2 Laboratory, Research & Innovation Center, Mitsubishi Heavy Industries, Ltd., Hyogo, 6768686, Japan

ryutaro@ruri.waseda.jp

Abstract. Generally, in industrial applications, multi-stage pumps are used to obtain high working pressure. However, utilizing these pumps requires larger body size and longer shafts which will lead to substantial costs. As a result, a low specific speed machine is needed to minimize costs. In such case, energy can be saved and manufacturing costs can be reduced by increasing the efficiency of these low specific speed machines disk friction loss is one important cause of friction in low specific speed machines. It is caused by fluid friction occurring in the clearances between the shroud and back-shroud of the impeller and the casing. This loss is not directly related to the energy conversion in turbo machines, however it is related to the main characteristics of a machine. It will be increased proportionally with the impeller diameter and decreased with its specific speed. In this research, a test apparatus for measuring friction torque on a rotating disk was established, including a pressure resistant tank and boost pump connected in a closed loop using water as the working fluid. The sample rotating disk simulated the leakage flow path between the back-shroud and the casing of a centrifugal pump. Disks with different clearances were prepared, and fluctuations of torque were studied as a function of flow rate and Reynolds number. As a result, an optimum value for disk clearance with the minimum torque was observed to exist under each flow condition. CFD analysis was performed using a model simulating the disk clearance to understand the internal flow structure. For purpose of validation, the radial distribution of static pressure on the stationary wall was simulated by CFD and compared to experimental results. The CFD analysis agreed with the experimental distribution of wall static pressure in an acceptable manner, therefore it is proved that CFD model can reliably be used in evaluation of disk friction loss. Moreover, disk friction loss variation as a function of flow rate was investigated with inward and outward flow directions. It is seen that for both directions, disk friction loss decreases with flow rate. However, a vortex structure was observed at the inlet of the disk clearance for inward flow direction. Size of the vortex structure changes as a function of flow rate and has an influence on disk friction loss. The occurrence of this vortex structure may increase the efficiency of actual low specific speed machinery.

1. Introduction

As disk friction loss is the main reason for efficiency drop in low specific pumps, its reduction will improve efficiency of centrifugal pumps. Disk friction loss is inherently caused by fluid friction

occurring in the clearance between the shroud and back-shroud of the impeller and the casing. This loss is not directly related to the energy conversion by the turbo machinery. It will be increased proportionally with an impeller diameter and decreased proportionally with its specific speed. [1] A common method for loss reduction is using riblet processing, which changes the characteristics of the disk. [2][3]

Measurement of disk friction loss is more satisfactory by experiments rather than CFD because meaningful computer analysis has not been conducted in literature. [4][5] Analysis of a narrow gap flow at rotating part requires a huge mesh number thus will results in calculation cost. [6] Therefore, trial-and-error methods are usually employed to find disk shapes for loss reduction. However, a theoretically predictable reduction method cannot exist as long as the detailed flow of the disc gap is not clarified.

In the current research, we conducted computational fluid dynamics (CFD) analysis to investigate the disk clearance flow for better understanding of disk friction loss. The analysis elucidates a large number of meshes by using periodic boundaries. The studied parameters for reduction of disk friction loss were flow direction, flow rate, and disc gap width. The results showed that disc gap width has an optimum value for minimizing disk friction loss. For purpose of validating the accuracy of computational analysis, an experimental apparatus was also constructed for measuring disc friction loss under the same conditions as CFD analysis. In addition, disk friction loss variation was investigated as a function of the flow rate with inward and outward flow directions. It is seen that for both directions, disk friction loss was decreased with magnitude of flow rate. However, a vortex structure was observed at inlet of the disk clearance for the inward direction flow. Size of this vortex structure changes as a function of flow rate and thus may have an influence on disk friction loss. The occurrence of this vortex structure may increase the efficiency of actual low-specific speed machinery.

1. Nomenclature

D	:	Diameter	[m]	N	:	Rotational speed	[min^{-1}]
D_{max}	:	Maximum diameter	[m]	ω	:	Angular velocity	[rad/s]
R	:	Radius	[m]	P	:	Wall static pressure	[Pa]
Q	:	Flow rate	[m^3/s]	Pa	:	P at outer measurement point	[Pa]
Q_1		Design flow rate	[m^3/s]	a	:	Radius at outer measurement point	[m]
S	:	Disk clearance	[m]	U	:	Disk peripheral velocity (=$\pi ND_{max}/60$)	[m/s]
S_1	:	Design disk clearance	[m]	u	:	Pre-rotation velocity	[m/s]
M		Disk friction moment	[Nm]	u_1	:	Outlet disk peripheral speed	[m/s]
ρ	:	Density	[kg/m^3]	V_{u1}	:	Outlet circumferential velocity	[m/s]
τ	:	Torque converted from angular momentum	[Nm]	u_2	:	Inlet disc peripheral speed	[m/s]
				V_{u2}		Inlet circumferential speed	

2. Test Apparatus

The test apparatus for measuring the friction torque generated on the disk is shown in Figure 2.1. The working fluid was water. The test part, the pressure resistant tank, and the boosting pump were connected in a closed circulation loop. The disc gap was fabricated by simulating a leakage flow path between the impeller back face of the centrifugal pump and the casing. The side and bottom of the test part were made of acrylic. Detailed analysis of flow field by optical measurement was possible. The pulley belt was driven by the servomotor and power could be transmitted to the disk. The pipes on the upper part of the test part were axially symmetrically connected at two places to cancel the distribution

in the circumferential direction. The tank was provided downstream of the pump discharge to suppress the influence of the pump, as shown in Figure 2.2. The gap flow could be directed outward and inward by changing the three-way valve installed in the pipe.

Figure 2.1 Experimental equipment.

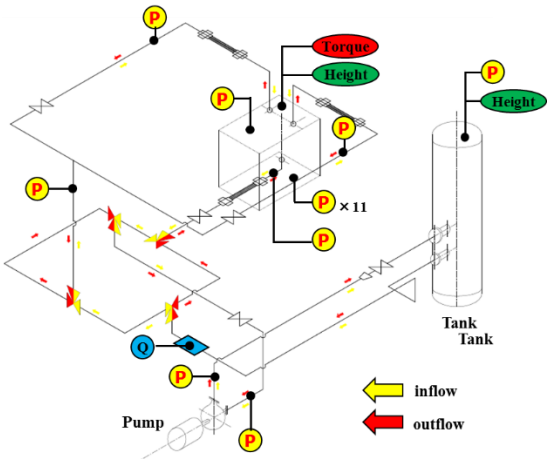

Figure 2.2 Piping isometrics.

The used parameters were the flow direction in the gap, the disk rotation speed, the flow rate, the axial gap ratio, and the surface finishing. The diameter of the disk was 380 [mm], and the axial gap ratio (S/S_1) was 0.4, 1, 2, and 5, as shown in Figure 2.3. Coating with alumite was carried out to improve corrosion resistance and abrasion resistance for disks. The parameters for the test were determined in the order of disc type, flow direction, flow rate, and disc rotation speed. Flow direction in the gap was changed by three-way valves, and the flow rate was adjusted by the pump rotational speed and the provided valve on the pump discharge. The disc rotation speed was adjusted through the control panel. The whole test apparatus was pressurized by a compressor to prevent cavitation at the pump suction-side piping and the lower part of the testing disk.

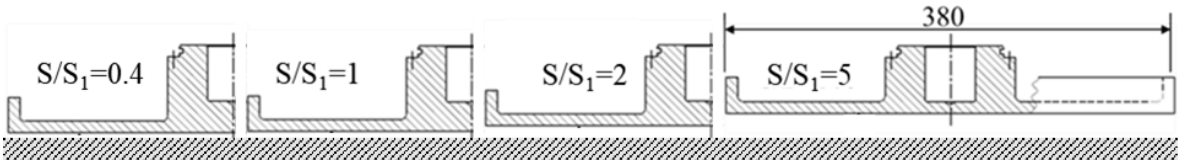

Figure 2.3 Axial clearance ratio.

A hollow shaft used for measuring torque was made from SUS 304, as shown in Figure 2.4. The position where the strain gauge was attached was processed on the shaft. A strain gauge lead wire was connected from the hollow portion to the slip ring. The strain gage was glued to the shaft, in which bending strain and tensile compressive strain on the shaft are eliminated. Two layers of rubber tape and adhesive were coated on the strain gauge to maintain insulation between the lead wire and water. As the tension of the shaft by the disc was not taken into consideration, the output represented only the torque.

The radial static pressure distribution on the static wall side was measured with a multipoint pressure transducer called DSA 3207. The pressure range was 0 to 30 psi (about 0.2 [MPa]). For measurement of pressure distribution, a polyurethane tube was used from the pressure measurement hole provided on the bottom of the specimen shown in Figure 2.5. Eleven measuring points existed every 10 mm from the point of radius 60 mm.

Figure 2.4 Hollow shaft.

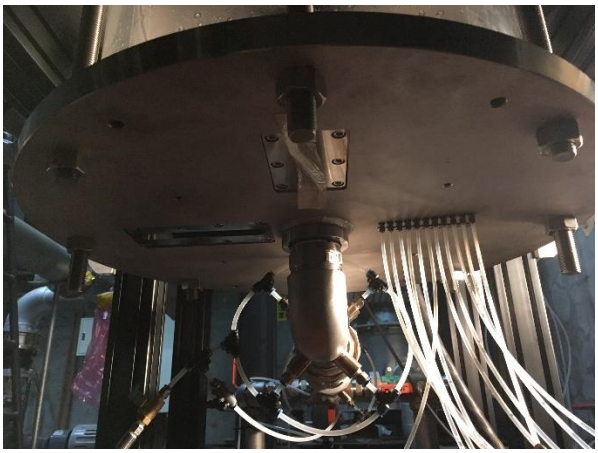

Figure 2.5 Hollow shaft and measuring points for pressure distribution.

3. Computational Framework

An analytical model used for studying the disk friction reduction method is shown in Figure 3.1. A parallel disk is used as a shape reproducing the disk gap. 400 meshes in the radial direction, 200 in the height direction and 50 meshes in the circumferential direction were created, which was structural grid meshes using ANSYS ICEM. Boundary layer thickness was set to 1×10^{-6}. The analysis conditions are shown in Table 3.1.

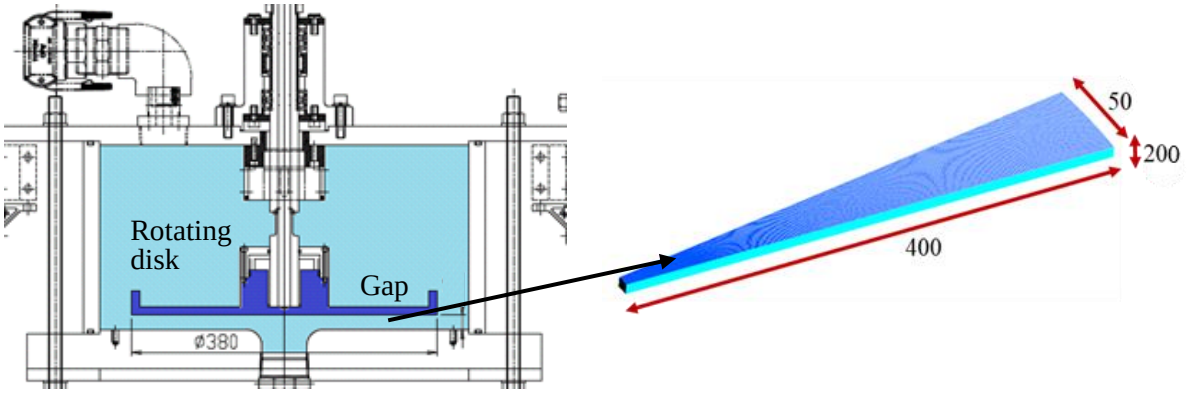

Figure 3.1 Mesh model.

Table 3.1 Conditions of CFD.

Code	ANSYS CFX 17.2
Method	RANS
Domain	Disc clearance
Inlet boundary	Constant mass flow rate
Outlet boundary	Opening Entrainment 0 [Pa]
Impeller speed	1000, 2000 [min-1]
Periodic boundary	9 [deg]
Flow direction	Inward/outward

4. Validation of numerical analysis

CFD analysis and experiment results were compared to establish the validity of the numerical analysis. Wall pressure coefficients C_p at each flow rate when the disk gap ratio S/S_1 = 0.4, 1.0, 5.0 are shown in Figure 4.1. Wall pressure coefficients C_p was defined as

$$C_P = \frac{P_0 - P}{1/2\rho\omega^2 a^2} \tag{1}$$

Where P_0, P, ρ, ω, a are static pressure at the outermost end of measurement hole, static pressure at measurement hole, density of water, disc angular velocity and radius at the outermost end of pressure measurement hole.

Static pressure distribution was measured at eleven points on the stationary wall side in the experiment. CFD accurately showed the tendency of the wall pressure as the flow rate is changed when S/S_1 = 0.4. The CFD results begin to deviate from the experimental results as the gap width increases due to the creation of a vortex in the internal structure. However, the influence of flow rate changes is correctly shown.

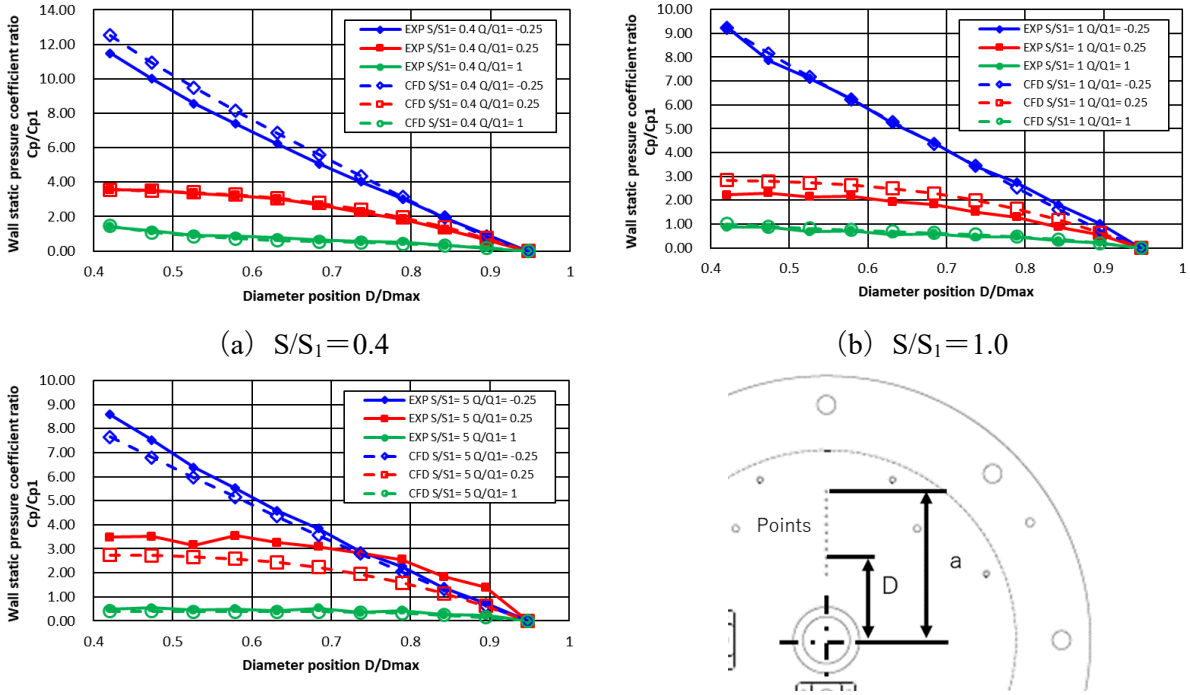

(a) S/S_1=0.4 (b) S/S_1=1.0

(c) S/S_1=5.0 (d) Measurement points

Figure 4.1 Wall pressure distribution.

Figure 4.2 shows the change in disk friction coefficient at different values of S/S_1. The negative and positive signs of flow rate indicate inward flow and outward flow respectively. Disk friction coefficient C_m was defined as [7]

$$C_m = \frac{2M}{\rho R^5 \omega^2} \tag{2}$$

Where M, ρ, R, ω are torque on disk, density of water, diameter of disc and angular velocity.

The value of S/S_1 at which the disk friction coefficient was minimized exists at all disk rotation speeds. The minimum value of S/S_1 obtained from the experiment was approximately S/S_1 = 1.0 % in the most of flow rates. Figure 4.3 shows the results of numerical calculations. At the test result $Q / Q_1 = 0$, the disk friction loss becomes minimum when $S / S_1 = 1$. The value of S/S_1 at which the disk friction

coefficient becomes the minimum existed. Despite variations in the trend of each result, the disk friction loss has inflection points around $S/S_1 = 1$. In $Q/Q_1 = 4$, the difference between CFD analysis and experimental results is large, but the tendency of loss to flow rate is the same. Therefore, influence on friction loss and internal pressure distribution were qualitatively captured by CFD analysis. This showed that the flow field could be predicted.

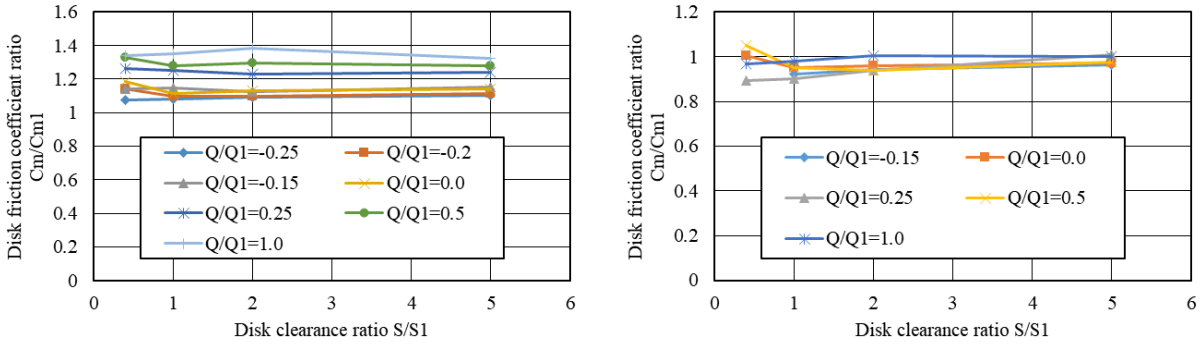

(a) Rotating speed 1000[min^{-1}] (b) Rotating speed 2000[min^{-1}]

Figure 4.2 experimental results of disk friction coefficient.

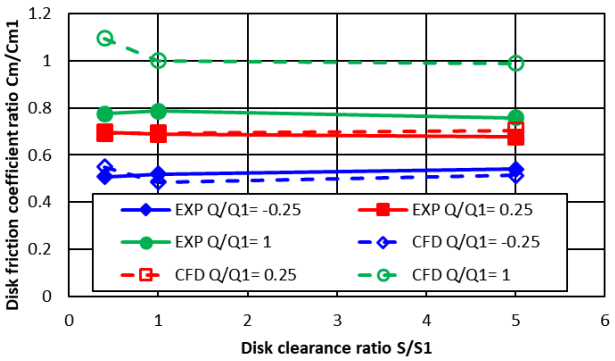

Figure 4.3 Effect of axial gap width and flow direction.

5. CFD Analysis

5.1. Influence of flow change

When the disk gap ratio $S/S_1 = 1$, analysis was performed with the flow rate as a parameter. The relationship between flow rate and disc friction coefficient C_m is shown in Figure 5.1, where the outward direction is positive and the inward direction is negative. The outward flow has a lower coefficient of friction of the disk when the flow rate is lower. The inward flow has an optimum value when the flow rate is around $Q/Q_1 = -0.125$.

Figure 5.2 shows a streamline contour of the inward and outward flow. They are cross section in the radial direction of the disk and the aspect ratio is changed for ease of visualizing. The top surface is the rotating wall and the bottom surface is the stationary one. The axis of rotation is on the left side. A vortex structure is seen in the disk gap at low flow rate and is not at high flow rate. This is because the vortex is flowed when the flow is fast, but it remains because it is late. Focusing on the inward flow vortex structure, the disk friction loss is smaller as the vortex size increases.

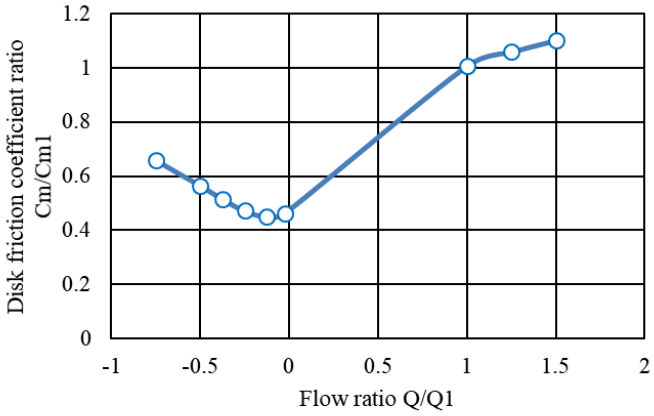

Figure 5.1 Relationship between flow rate and disc friction coefficient.

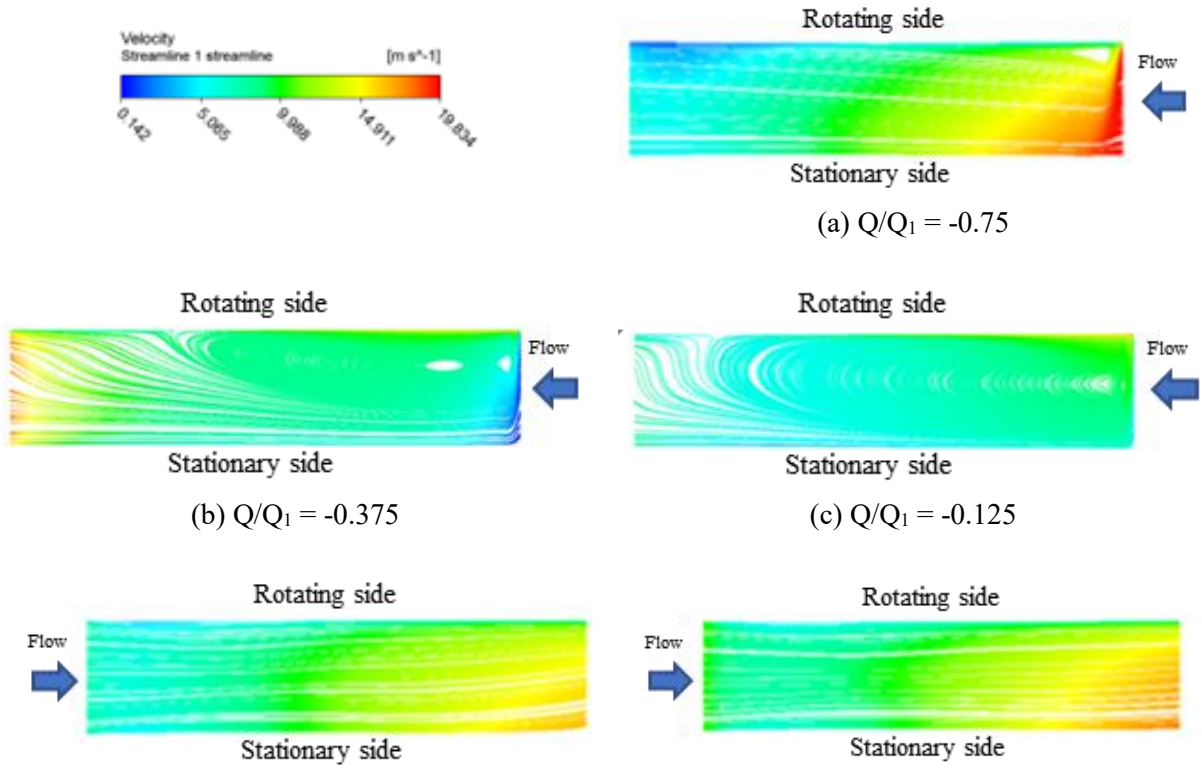

Figure 5.2 Streamline contour.

5.2. Influence of pre-rotation

CFD analysis was performed by giving entrance pre-rotation in a flat plate model. The pre-rotation was given in the forward direction respect to the direction of rotation of the disk. It was set to 1/4 U, 2/4 U, 3/4 U with respect to the circumferential speed U at disk outer diameter. Table 5.1 shows detailed analysis parameters.

Figure. 5.3 shows a graph of the results of disk friction coefficients corresponding to each pre-rotation in inward flow and outward flow. As is apparent from the graph, the disk friction coefficient was reduced by giving the entrance pre-rotation in both inward and outward conditions. In outward flow,

the change in disk friction coefficient due to swirl is constant and linear. On the other hand, in inward flow, the graphs are not parallel. Therefore, the outward flow is influenced simply by increasing the angular momentum of the entrance. However, inward flow has an influence other than increase of angular momentum.

The difference between the inlet angular momentum and the outlet angular momentum is the torque that fluid exerts on the disc. When the entire disk gap is set as the inspection volume, the fluid works on both sides of the rotating wall and the stationary wall shown as Figure 5.4. Then, Figure 5.5 shows four data as:

1. Disk friction coefficient on the rotating wall (CFD)
2. Disk friction coefficient on the stationary wall (CFD)
3. Disk friction coefficient on the rotating and stationary wall (CFD)
4. The difference between the inlet angular momentum and the outlet angular momentum

4 was defined as

$$\tau = \frac{\rho Q}{\omega}(u_1 \cdot V_{u1} - u_2 \cdot V_{u2}) \tag{3}$$

In the inward flow, the torque value on the stationary wall side is sufficiently larger than the angular momentum. The torque on the stationary wall side strongly influences the torque value on the rotating wall side. the torque on the rotating wall side can be reduced by increasing the torque on the rotating wall side. Figure 5.6 shows a streamline contour of the inward with pre-rotation. As shown in Figure 5.6, the vortex structure becomes bigger with increasing pre-rotation. In other words, as shown in Figure 5.7, as the vortex grows bigger, the velocity gradient on the side of the rotating wall decreases and the velocity gradient on the side of the stationary wall increases. Therefore, the torque value on the stationary wall side increases, and the torque value on the rotating wall side decreases.

Table 5.1 Parameters of CFD.

Flow direction	Q/Q_1	N	u/U
inflow	-0.25	1000	0.25
inflow	-0.25	1000	0.5
inflow	-0.25	1000	0.75
outflow	1	1000	0.25
outflow	1	1000	0.5
outflow	1	1000	0.75

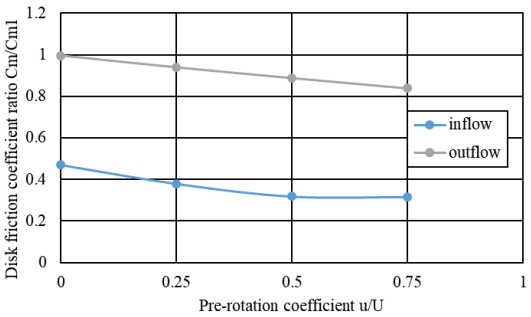

Figure 5.3 Disk friction depend on pre-rotation.

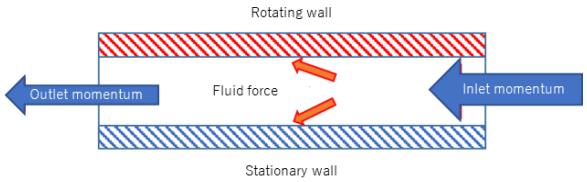

Figure 5.4 Conceptual diagram.

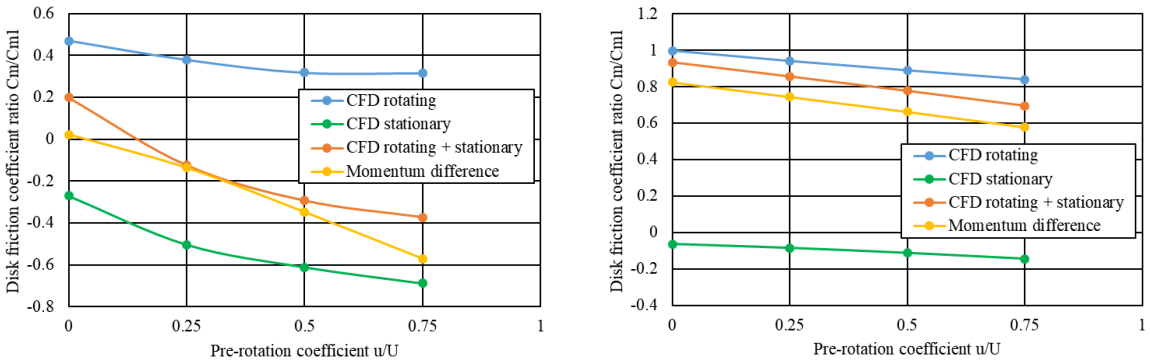

(a) $Q/Q_1 = -0.25$ (b) $Q/Q_1 = 1$

Figure 5.5 Disk friction and angular momentum.

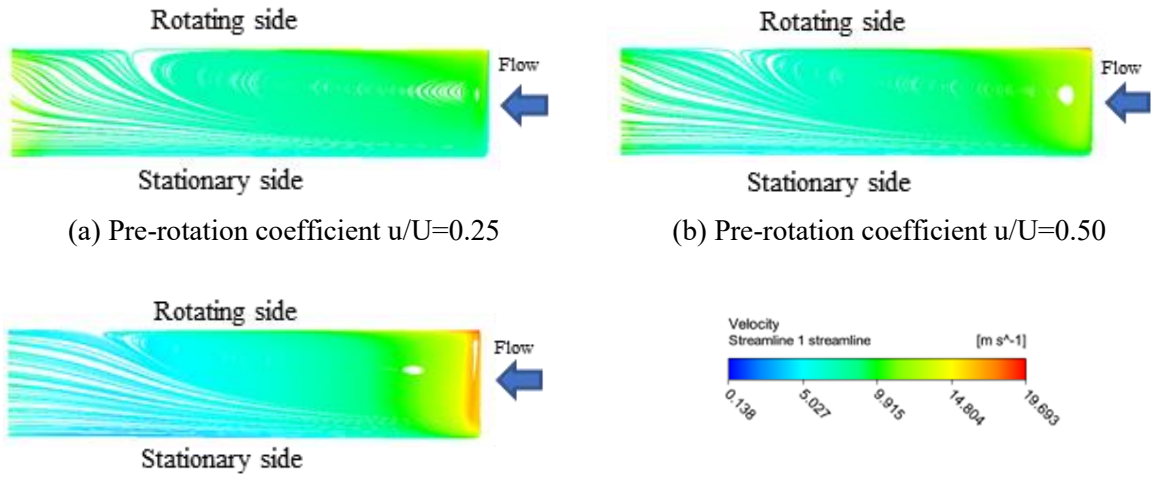

(a) Pre-rotation coefficient u/U=0.25 (b) Pre-rotation coefficient u/U=0.50

(c) Pre-rotation coefficient u/U=0.75

Figure 5.6 Streamline contour (Q/Q_1=-0.25).

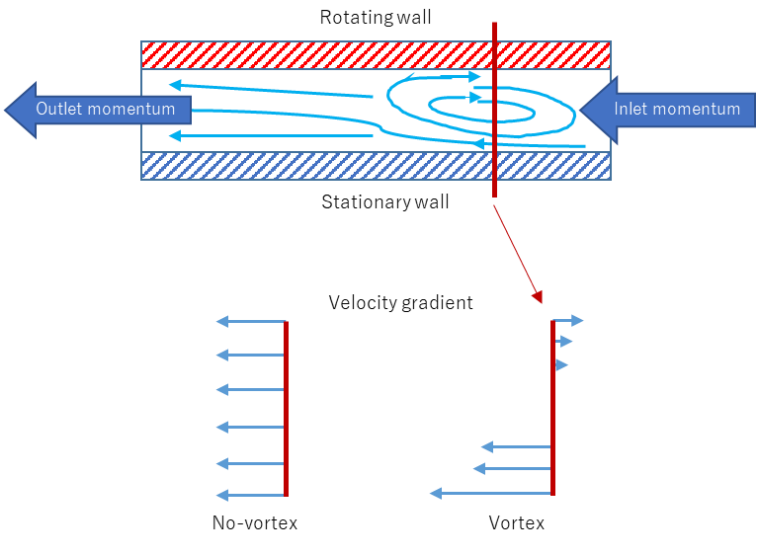

Figure 5.7 Velocity gradient on the rotating and stationary wall.

6. Conclusion

The main outcomes of the current research are as follows:

(1) A disk friction experiment setup was constructed, and many experiments have been performed to measure pressure distribution in radial direction of the disk and the rotating torque of the disk.
(2) The optimum value of disk friction coefficient for S/S_1 exists under each flow rate condition.
(3) The result of the CFD analysis was confirmed to agree with the experimental results qualitatively by comparing the pressure distribution in the radial direction
(4) The outward flow has smaller disk friction coefficient as the flow rate becomes smaller.
(5) Pre-rotation given into the clearance inlet decreased disk friction coefficient in both inward and outward flow.
(6) The CFD analysis confirmed vortex structures in the disk clearances.

Acknowledgement

The authors would like to thank the Waseda Research Institute for Science and Engineering (WISE) for providing support to the presented research, in context of the project: 'High performance and high reliability research for hydraulic turbomachinery systems'.

References

[1] Mikhail, S., M. G. Khalafallah, and M. El-Nady. "DISK FRICTION LOSS IN CENTRIFUGAL AND MIXED FLOW PUMPS." *7th International Congress on Fluid Dynamics and Propulsion*. 2001.
[2] M.J.,"Turbulent boundary layer drag reduction using riblets"AIAA,82-0169,(1982).
[3] Matsumoto, Kazunari, et al. "Performance improvement and peculiar behavior of disk friction and leakage in very low specific-speed pumps." Nihon Kikai Gakkai Ronbunshu, B Hen/Transactions of the Japan Society of Mechanical Engineers, Part B 65.640 (1999): 4027-4032.
[4] Nemdili, A., and D. H. Hellmann. "Investigations on fluid friction of rotational disks with and without modified outlet sections in real centrifugal pump casings." Forschung im Ingenieurwesen 71.1 (2007): 59-67.
[5] Gülich, J. F. "Disk friction losses of closed turbomachine impellers." *Forschung im Ingenieurwesen* 68.2 (2003): 87-95.
[6] Mohammadreza Daqiqshirazi, Alireza Riasi, Ahmad Nourbakhsh. "NUMERICAL STUDY OF FLOW IN SIDE CHAMBERS OF A CENTRIFUGAL PUMP AND ITS EFFECT ON DISK FRICTION LOSS." International Journal of Mechanical And Production Engineering. Volume- 2, Issue- 3, (2014).
[7] Watanabe, Keizo, Satoshi OGATA, and Keigo UEMURA. "Drag reduction of an enclosed rotating disk with fine spiral grooves." Journal of Environment and Engineering 2.1 (2007): 97-107.